RAPID COMMUNICATIONS

PHYSICAL REVIEW B VOLUME 42, NUMBER 17 15 DECEMBER 1990-I

Molecular-beam-epitaxial growth and magnetic properties of Co-Pt superlattices oriented along the [001], [110], and [111] axes of Pt

C. H. Lee, R. F. C. Farrow, C. J. Lin, and E. E. Marinero
IBM Research Division, Almaden Research Center, 650 Harry Road, San Jose, California 95120-6099

C. J. Chien
Department of Materials Science and Engineering, Stanford University, Stanford, California 94305
(Received 24 September 1990)

We report the growth of Co-Pt superlattices along three different crystalline orientations of Pt by molecular-beam epitaxy. [001], [110], and [111] orientations of Co-Pt superlattices were grown using seeded epitaxy techniques on GaAs substrates. The room-temperature magnetic properties are strongly different for the three orientations. Structural analysis of the superlattices reveals significant differences in interface quality and defect structure for the three different orientations. These effects may play a more important role in the origin of magnetic anisotropy than previously assumed.

Artificially layered magnetic metal structures, including superlattices, are a topic of intense current interest because of their unusual properties and potential device applications. Indeed, these structures have, in the past few years, demonstrated[1] a variety of phenomena such as large perpendicular anisotropy, giant magnetoresistance, and Ruderman-Kittel-Kasuya-Yosida (RKKY) coupling. As observed in several magnetic systems, Co-Au,[2] Co-Cu,[3] Fe-Ag,[4] Co-Pt,[5] and Co-Pd,[6] a perpendicular easy axis of magnetization can be achieved when the magnetic layer thickness is smaller than a few monolayers. Interfacial anisotropy has been used to describe this effect but its origin remains unclear. Although there are indications that the magnetic and structural properties are closely related, the understanding has been hampered by the difficulty in obtaining well-defined single-crystal structures. For example, for the Fe/Ag (Refs. 4 and 7) and Co/Pd (Ref. 6) systems it has been shown that different anisotropies can be obtained for different crystalline orientations of the ferromagnetic film. However, this result is not clear cut because the comparison is not between single-crystal films grown under identical conditions in the same growth chamber. Molecular-beam epitaxy (MBE) growth of a particular materials system under identical conditions is necessary for a clear-cut comparison. The technique of seeded epitaxy by MBE (Ref. 8) is a route to such a comparison since it enables the orientation of a superlattice to be controlled, keeping other growth conditions constant. In addition, it permits *in situ* structural characterization at all stages of film growth. In this paper, we report the MBE growth of Co/Pt superlattices along three crystal orientation selected by growth on suitably prepared GaAs substrates. We find that the magnetic properties of the superlattices are reproducible and strongly dependent on the superlattice growth orientation.

Co-Pt superlattices prepared by sputtering and conventional evaporation techniques have been shown[5,9] to have preferred texture along the [111] orientation of Pt. Such structures have an easy axis of magnetization along this axis when the Co layer thickness is smaller than ~ 10 Å.[5,9] Such Co/Pt superlattices have a significant Kerr rotation at GaAs laser wavelengths and exhibit an increase in Kerr rotation with decreasing wavelength.[9] The figure of merit for magneto-optical data readout is greater[9] for these superlattices than for the amorphous rare-earth transition-metal alloys, especially at shorter wavelengths. As a result, Co/Pt superlattices are promising as media for magneto-optical recording.[9] The origin of the perpendicular anisotropy in these structures, however, remains unexplained. In a related study, den Broeder *et al.*[6] have examined the effect of the growth axis of Co/Pd superlattices on magnetic anisotropy. They found that the crossover thickness was orientation dependent for this system but their comparison was between [111] textured polycrystalline superlattices on glass and epitaxial [001]-oriented superlattices grown on NaCl substrates. These authors did not present data on x-ray diffraction from the polycrystalline structures so the angular dispersion of the growth axis in this case was not defined. The possible presence of mixed orientations of the superlattice growth axis prevents a definitive comparison between the data. Furthermore, since no low-angle x-ray-diffraction data from either of the structures was presented, the extent of interdiffusion and interfacial mixing in the two cases remains unclear. In the present study we have used the technique of seeded epitaxy[8] to define uniquely the growth axis of the Co/Pt superlattices along the three major directions of Pt and have also studied both the low- and high-angle x-ray diffraction from the structures to determine the quality of the layering.

The Co-Pt superlattices reported in this Rapid Communication were prepared in a VG 80-M MBE system (VG Semicon Ltd.). Two orientations of GaAs substrates were used to seed the different superlattice orientations. For the case of [001] and [110] orientations, we used substrates with MBE-grown buffer layers of homoepitaxial GaAs(001). The surface of the substrates was inclined at $\lesssim 0.1°$ to the (001) plane. Following GaAs epitaxy, the surface was capped by an overlayer of arsenic which was deposited at ~ -20 °C. The substrates were kept in a

vacuum flask between the two MBE growth cycles. Just before superlattice growth, the substrate was heated to $\sim 500\,^{\circ}C$, in a background pressure of $\sim 10^{-10}$ mbar to remove the arsenic cap. This generated a clean, ordered, As-stabilized (1×1) or (2×4) surface. The nature of this surface reconstruction did not influence the result of this study. For superlattice growth along the Pt [111] direction, substrates cut with the surface normal within $\sim 0.5^{\circ}$ of the $[\bar{1}\,\bar{1}\,\bar{1}]$ direction were used. The substrate surface was prepared by chemical-mechanical polishing and subsequent etching in a 1:1:100 solution of H_2O_2/NH_4OH/H_2O. Heating of the substrate to $\sim 600\,^{\circ}C$ in a background pressure of $\lesssim 10^{-10}$ mbar was used to remove surface impurities and to generate a 1×1 reflection high-energy electron diffraction (RHEED) pattern.

The Co and Pt layers were grown from *e*-gun sources at rates of ~ 0.15 and ~ 0.25 Å/sec, respectively. The deposition rates and beam-interrupt shutters were computer controlled using a Sentinel III deposition control system (Leybold Heraus Inc.). Fluctuations in film thickness were less than 2%. Ag layers were grown at a rate of 0.35 Å/sec from a Knudsen cell held at $\sim 1050\,^{\circ}C$. The background pressure prior to film growth was approximately $\sim 2\times10^{-11}$ mbar, while the pressure during superlattice growth was $\sim 2\times10^{-10}$ mbar or lower.

The key to successful Co-Pt superlattice growth in the three different orientations hinges on the initial epitaxy of Ag. The Ag film seeds parallel epitaxy of the isostructural Pt film in each orientation and controls the orientation of the entire superlattice.

RHEED patterns were recorded during growth of each of the superlattices. Figure 1 shows RHEED patterns representative of growth of the three orientations. The patterns shown are from the initial GaAs surface, Ag, and final Pt films. In the case of the [110] oriented superlattice, additional RHEED patterns are shown from the first Pt and Co films. The [111] orientation of Co-Pt superlattices was selected by first depositing ~ 200 Å of Ag onto the clean GaAs substrate at a substrate temperature of $100\,^{\circ}C$. RHEED [see Fig. 1(a)] and low-energy electron diffraction (LEED) studies showed that the Ag grew with its (111) plane parallel to the GaAs(111) plane. The sixfold symmetry patterns observed in RHEED and at all energies in LEED were consistent with rotational twinning of the Ag film by 180° about the [111] axis. This was subsequently confirmed by x-ray diffraction and transmission electron diffraction. The Co/Pt superlattice was then grown with the Pt film deposited first. The superlattices contained 7 or 15 periods and were capped with a 16-Å Pt film to stabilize the surface against atmospheric oxidation. The entire superlattice followed the rotational twinning of the initial Ag film:

$$\text{Ag, Pt}(111),\ [0\bar{1}1]\|\text{GaAs}(\bar{1}\,\bar{1}\,\bar{1}),\ [0\bar{1}1],$$

$$\text{Ag, Pt}(111),\ [01\bar{1}]\|\text{GaAs}(\bar{1}\,\bar{1}\,\bar{1}),\ [0\bar{1}1].$$

The [110] oriented Co-Pt superlattices were prepared by first heating the GaAs to about $\sim 500\,^{\circ}C$ to remove the As layer. The substrate was then cooled to $\sim 100\,^{\circ}C$ and then 200 Å of Ag deposited. Immediately after deposition, the Ag RHEED pattern indicated a rough surface with short diffuse streaks consistent with Ag(110). Annealing the surface, *in situ,* for about two hours at $100\,^{\circ}C$ resulted [see Fig. 1(b)] in a lengthening and sharpening of the RHEED streaks and a 4×1 reconstruction. This indicates that the annealing resulted in smoothing of the surface and a well-defined orientation of Ag(110). Co-Pt superlattices were then grown on the surface at $100\,^{\circ}C$. The

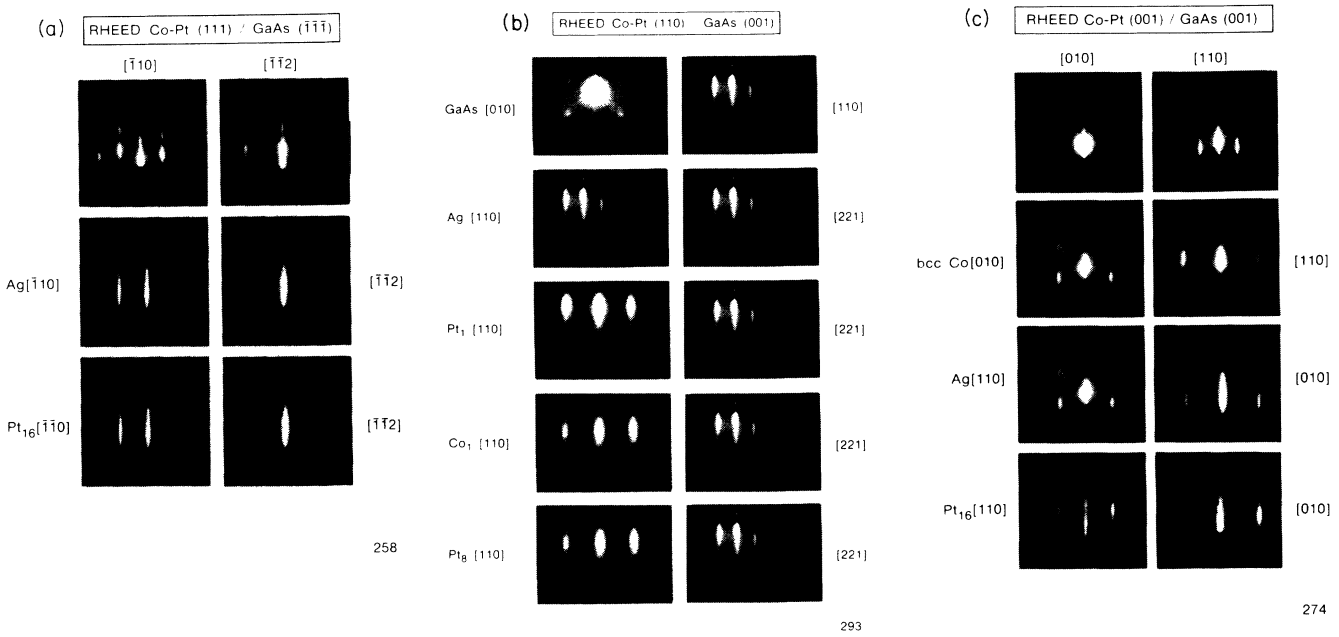

FIG. 1. RHEED patterns recorded during seeded epitaxy of Co/Pt superlattices along (a) [111], (b) [110], and (c) [001] directions of Pt. The electron energy was 14 keV. Note the sharp and well-defined streaks persisting to the final Pt capping film for all orientations. See text.

epitaxial relations determined from the RHEED and LEED data were

$$\text{Ag}(110), [\bar{1}10] \| \text{GaAs}(001), [100].$$

No twinning was present in any of the [110] oriented superlattices.

The [001] oriented superlattices were grown on Ag(001) surfaces produced by Ag deposition on thin (~3–9 monolayers) Co seed films. These seed the epitaxial growth of Ag along the [001] axis. The Co prelayer adopted[10] a body-centered tetragonal structure, commensurate in plane with the GaAs [001] substrate. The Ag film grew epitaxially on the Co rotated in plane by 45°:

$$\text{Ag}(001), [100] \| \text{Co}(001), [110] \| \text{GaAs}(001), [110].$$

The Co-Pt superlattice was then grown, starting with the Pt film.

No twinning was present in any of the [001] oriented superlattices. The magnetic signal from the Co seed film was measured and found to be negligible compared with the magnetization from the superlattices. This suggests that the Co may have a reduced moment from chemical interaction with the substrate, as previously indicated by Prinz[11] for Fe on GaAs(110).

X-ray-diffraction measurements were carried out on a double-crystal diffractometer with a GaAs(111) plane monochromator operating in the (111) Bragg diffraction. The Cu $K\alpha_1$ line was selected by a slit. These measurements were made to determine the period of the superlattices from satellite peak positions, the quality of the interfaces, and whether the superlattice growth axis was singular. High- and low-angle θ-2θ scans were made in the symmetric reflection geometry and examples are shown in Figs. 2 and 3 for [111] and [001] oriented superlattices of 15 periods with Co film thicknesses of 3.2 and 3.7 Å, respectively. The Pt film thickness was 16.8 Å in both cases. The $n=0$ superlattice peak, which occurs at the Bragg angle corresponding to the average lattice spacing for one period, was found at 2θ values of 40.24°, 47.32°, and 68.7° for the [111]-, [001]-, and [110]-oriented superlattices. These angles are in agreement with the predicted peak positions for these orientations and no other orientations were found, i.e., the orientations were mutually exclusive. For all three orientations, Bragg peaks from the GaAs substrate, Ag seed film, and the superlattice were observed. The superlattice period determined from the superlattice peak positions agreed within 2% of the period determined from the Co and Pt thickness calibrations. It can be seen from Fig. 2 that the [001]-oriented superlattice has a slower falloff in intensity of the higher-order satellite peaks than for the [111]-oriented superlattice. This suggests that the [001] superlattice has better defined interfaces than the [111] case. This view is supported by the low-angle x-ray-scattering data shown in Fig. 3. It is clear that the [111] structure has a much more rapid falloff of satellite intensities. In fact the third-order satellite is almost negligible for this orientation. Modeling of the low-angle x-ray reflectance, using an x-ray multilayer code,[12] shows that the data for [111] can be fitted if considerable interface compositional mixing is assumed. A linear grading length of 3 Å gives a close fit to the data.

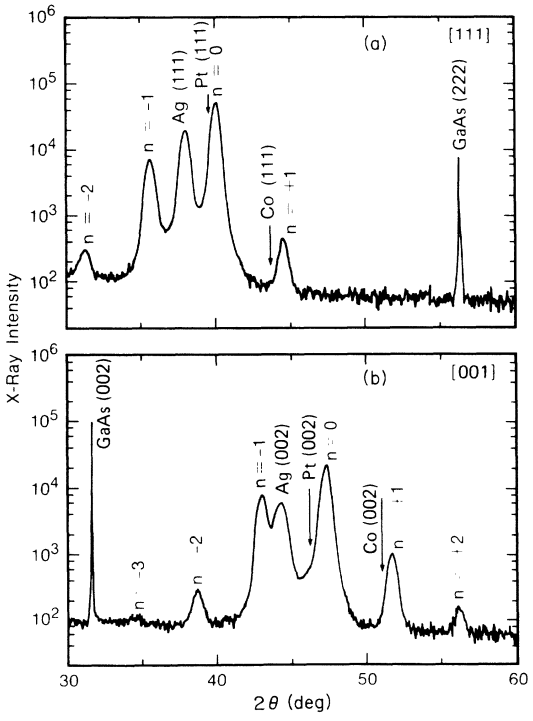

FIG. 2. High-angle x-ray-diffraction θ-2θ scan for [111]- and [001]-oriented superlattices comprising: (a) GaAs($\bar{1}\bar{1}\bar{1}$)/[200Å Ag(111)]/[16.8 Å Pt–3.2 Å Co]$_{15}$/(16.8 Å Pt); (b) GaAs($\bar{1}\bar{1}\bar{1}$)/(10 Å Co)/[200 Å Ag(001)]/[16.8 Å Pt–3.7 Å Co]$_{15}$/(16.8 Å Pt).

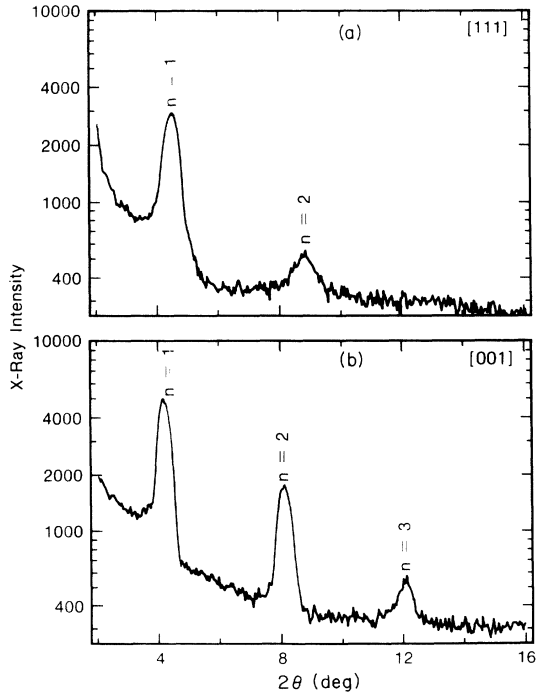

FIG. 3. Low-angle x-ray-diffraction θ-2θ scan for same superlattices as Fig. 2.

This implies that the superlattice does not contain pure Co but is rather a compositionally modulated structure comprising graded transitions between a Co-Pt alloy and Pt. On the other hand, the data for the [001] and [110] structures are consistent with a mole abrupt profile.

High-resolution transmission electron microscopy (HRTEM) studies have been carried out on the superlattices to determine the microstructure of the samples. These results will be discussed in detail elsewhere.[13] The data confirm the epitaxial relations determined from the RHEED and x-ray-diffraction studies. They also reveal structural differences between the different orientations. For all three orientations the stacking within the superlattice is fcc. This is expected from the fcc structure of Pt and the large Pt/Co ratio. Additionally, stacking faults on the (111) planes were a common defect for the [111] oriented superlattices but were not observed for the other orientations. Furthermore, a high density of steps in the (111) planes of the [111] oriented superlattices was indicated[14] by the existence of symmetry-forbidden Bragg peaks such as $\frac{1}{3}(4\bar{2}\bar{2})$.

Room-temperature magnetic measurements were made on the superlattices using the polar Kerr effect ($\lambda = 633$ nm), vibrating sample magnetometry, and torque magnetometry. Figure 4 shows the results of the perpendicular Kerr measurements for the three different orientations, 15-period superlattices, each of the composition $\simeq 3$ Å Co–16.8 Å Pt. The [111] sample exhibits a highly square loop with a coercivity of 3.2 kOe. This sample has remanent magnetization perpendicular to the film plane. On the other hand, the [001] sample has no remanence and cannot be saturated at the highest field (16 kOe) we have used. This clearly indicates strong in-plane anisotropy. The [110] sample has intermediate behavior with small remanence both in plane and out of plane of the film.

In summary, we have demonstrated single-crystal growth of Co/Pt superlattices along three orientations and observed distinctly different magnetic anisotropy. In addition, our x-ray and TEM analysis indicates differences between the orientations in interface abruptness and defect structure. Therefore it is apparent that the origin of the perpendicular anisotropy observed in these superlattices cannot be accounted for by surface anisotropy and broken-symmetry arguments alone. However, epitaxy along these different orientations can clearly induce defect structures and local lattice distortions that may result in different values of the magnetocrystalline anisotropy. These effects may play a more important role in the origin of magnetic anisotropy than previously assumed

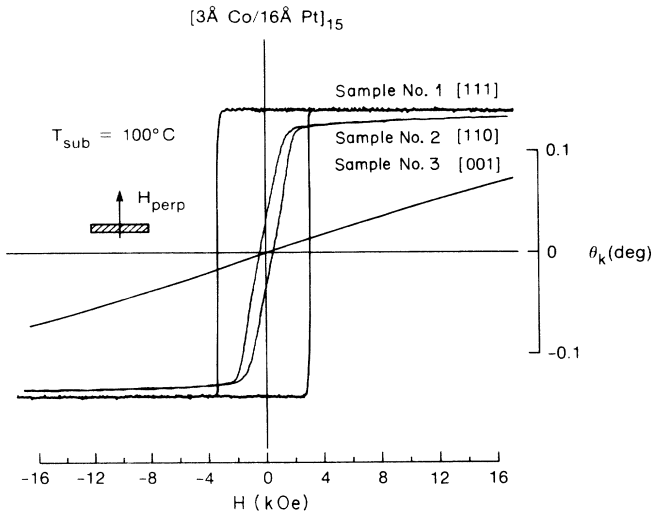

FIG. 4. Magnetic hysteresis loops recorded at 20 °C by Kerr rotation for oriented Co/Pt superlattices with ($\simeq 3$ Å Co–16.8 Å Pt)×15 periods. Wavelength of incident laser 633 nm. The magnetic field was applied normal to the sample surface.

This work was supported in part by the U.S. Office of Naval Research Contract No. N00014-87-C-0339.

[1]For a comprehensive current review of the field of magnetism in artificially layered magnetic films, see Appl. Phys. A **49**, 437 (1989); **49**, 547 (1989).

[2]C. Chappert, K. Le Dang, P. Beauvillain, H. Hurdequint, and D. Renard, Phys. Rev. B **34**, 3192 (1986); C. H. Lee, Hui He, F. Lamelas, W. Vavara, C. Uher, and Roy Clarke, Phys. Rev. Lett. **62**, 653 (1989).

[3]D. Pescia, G. Zampieri, M. Stampanoni, G. L. Bona, R. F. Willis, and F. Meier, Phys. Rev. Lett. **58**, 933 (1987); F. J. Lamelas, C. H. Lee, Hui He, W. Vavra, and Roy Clarke, Phys. Rev. B **40**, 8 (1989).

[4]N. C. Koon, B. T. Jonker, F. A. Volkening, J. J. Krebs, and G. A. Prinz, Phys. Rev. Lett. **59**, 2463 (1987); J. R. Dutcher, J. F. Cochran, B. Heinrich, and A. S. Arrott, J. Appl. Phys. **64**, 6095 (1988).

[5]W. B. Zeper, J. A. M. Greidanus, P. F. Carcia, and C. R. Fincher, J. Appl. Phys. **65**, 4971 (1989).

[6]F. J. A. den Broeder, D. Kuiper, H. C. Donkersloot, and W. Hoving, Appl. Phys. A. **49**, 507 (1989).

[7]Z. Q. Qiu, S. H. Mayer, C. J. Gutierrez, H. Tang, and J. C. Walker, Phys. Rev. Lett. **63**, 1649 (1989).

[8]R. F. C. Farrow, V. S. Speriosu, S. S. P. Parkin, C. Chien, J. C. Bravman, R. F. Marks, P. D. Kirchner, G. A. Prinz, and B. T. Jonker, in *Thin Films: Stresses and Mechanical Properties,* edited by J. C. Bravman, W. D. Nix, D. M. Barnett, and D. H. Smith, MRS Symposia Proceedings No. 130 (Materials Research Society, Pittsburgh, 1989), p. 281.

[9]Shunichi Hashimoto, Y. Ochiai, and K. Aso, J. Appl. Phys. **67**, 2136 (1990).

[10]High-resolution, cross-sectional transmission electron microscopy of the Co-GaAs interface region confirmed in-plane coherency between the GaAs, Co, and Ag lattices but also revealed a tetragonal distortion of the Co lattice.

[11]G. A. Prinz, in *Thin Film Growth Techniques for Low Dimensional Structures,* edited by R. F. C. Farrow, S. S. P. Parkin, P. J. Dobson, J. H. Neave, and A. S. Arrott, NATO Advanced Study Institutes, Series B Vol. 163 (Plenum, New York, 1987), p. 313.

[12]S. Mrowka, Oxford Applied Research Group.

[13]C. J. Chien, C. H. Lee, R. F. C. Farrow, C. J. Lin and E. E. Marinero, *Proceedings of European Materials Research Society Spring Conference, Symposium C, 1990* [J. Magn. Magn. Mater (to be published)].

[14]J. M. Gibson, M. Y. Lazerotti, and V. Elser, Appl. Phys. Lett. **55**, 1394 (1990).

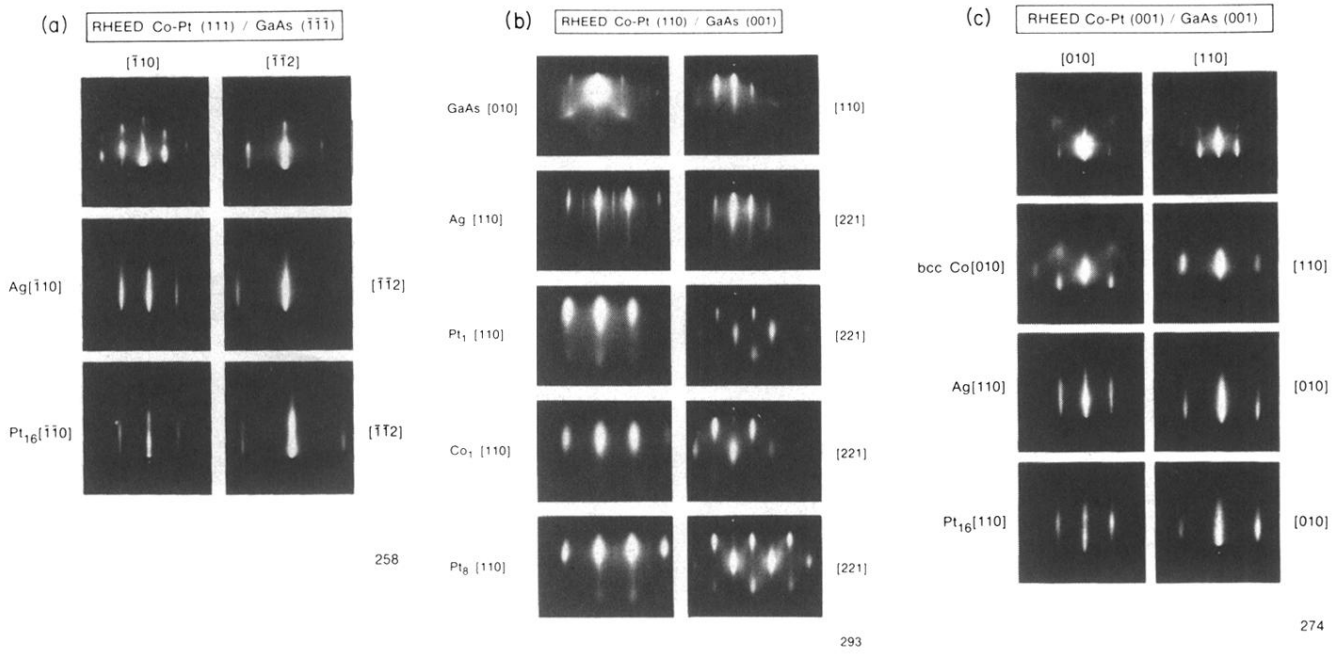

FIG. 1. RHEED patterns recorded during seeded epitaxy of Co/Pt superlattices along (a) [111], (b) [110], and (c) [001] directions of Pt. The electron energy was 14 keV. Note the sharp and well-defined streaks persisting to the final Pt capping film for all orientations. See text.